2011 IEEE/RSJ International Conference on
Intelligent Robots and Systems
September 25-30, 2011. San Francisco, CA, USA

Human-like Walking with Toe Supporting for Humanoids

Kanako Miura, Mitsuharu Morisawa, Fumio Kanehiro, Shuuji Kajita, Kenji Kaneko and Kazuhito Yokoi

Abstract— **A model of a walking pattern imitating human motion is presented. An accurate imitation of human motion and a robust bipedal walking motion are, however, hardly realized together. We therefore focus on only three characteristics of human walking motion: single toe support, knee stretching, and swing leg motion. Based on a conventional pattern generator, single toe support is added, waist height is changed in order to stretch the knees as much as possible, and swing leg motion is generated approximating the human's motion. The generated motion is then filtered to provide a feasible pattern. In addition, the stabilizer is improved in order to keep the Zero Moment Point (ZMP) within the tiny support polygon during the single support phase with toe link. Finally, we successfully demonstrate the generated walking pattern with the robot HRP-4C.**

I. INTRODUCTION

HRP-4C [1] was first shown to the public in March, 2009. The primary use of this robot was entertainment, such as acting as master of ceremonies at an event or as a model in a fashion show. HRP-4C had already been used in such events in an effort to clarify its usefulness for entertainment purposes [2]. Since HRP-4C had been designed to meet such entertainment needs, the height (158 cm) and length of the body links were based on the measured average of 19- to 29-year-old women in Japan [3]. On the other hand, emphasizing convenience in its operation on-site, it weighed only 43 kg when it was first released to the press. This weight included the battery, which was 10 kg lighter than average.

Through our demonstrations at such events, we received many requests and realized the need for improvements. For example, the ability to walk with a humanlike bipedal motion is necessary for events such as a fashion show. HRP-4C, however, walks with our conventional pattern generator, which is quite different from human motion. The hardware improvements have therefore been done and the main modification was adopting a new foot with a toe joint [4]. We also developed a new walking pattern generator, dynamics filter, and stabilizer as a part of a comprehensive approach to making HRP-4C walk like a human by using the toe joints, which is presented in this paper.

The rest of this paper is organized as follows. Related works are mentioned in the next section. After presenting the characteristics that we focus on in order to realize a human-like walking motion in Section III, the procedure of generating the walking patterns of a robot is described in Section IV. The generated pattern is modified to improve its dynamical feasibility in Section V, and in the next section we describe how the error of the robot's model was compensated for in real-time by the stabilizer. We examine the generated motion with a real humanoid robot HRP-4C and the walking motion is successfully demonstrated in Section VII. We conclude this paper and address our future plans in the last section.

All authors are with Humanoid Research Group, Intelligent Systems Research Institute, National Institute of Advanced Industrial Science and Technology (AIST), 1-1-1 Umezono, Tsukuba, Ibaraki, 305-8568, Japan kanako.miura, m.morisawa, f-kanehiro, s.kajita, k.kaneko, kazuhito.yokoi@aist.go.jp

II. RELATED WORKS

The question "With a robot, what gives an impression of human-likeness to observers?" is difficult to answer.

In the field of psychophysics, an investigation revealed that human can recognize human walking motion only watching the motion of several point-lights [5]. Moreover, human can distinguish different walkers [6] [7]. There is also a research to identify the factors contributing viewer's impression such as "male-female" or "happy-sad", and the modification of point-light walking motion according to the impression word is demonstrated on the web [8] [9]. In the field of robotics, motion capture data is used for measuring similarity to an arbitrary "reference pose" [10]. Producing realistic motion of a robot with human figure is well discussed in papers addressing dynamic feasibility and naturalness [11] [12] [13]. Human walking and humanoid walking are compared in order to apply the human walking functions to the humanoid robots [14]. The former (field of psychophysics) mainly focused on human perception, and the latter (field of robotics) focused on the conformity of data. From an intermediate standpoint, congruity between human perception and captured data about similarity of walking motions has been investigated [15].

Many researchers working on bipedal walking motion of humanoid robots have tried to answer this question by demonstrating using their own separate methods. WABIAN-2/LL was the first succeess, with a knee stretch walking motion in which the singularity of the swing leg is avoided by using waist joints [16]. The researchers also realized heel-contact and toe-off motion with WABIAN-2R, which had two 1-degree-of-freedom (DOF) passive toe joints [17]. Instead of using waist joints, Jaemi HUBO relied on a system of posture controls consisting of body-balancing and vibration-reduction units [18].

Similarity with human or naturalness of a motion was often evaluated by the degree of coincidence with motion-capture data. From this viewpoint, a few studies demonstrated on a human-size bipedal robot: Japanese traditional dance [19], Chinese Kungfu [20], and simultaneous capturing and imitation of whole-body motion [21] have been realized. However the human motion references were normally very

978-1-61284-455-8/11/$26.00 ©2011 IEEE

slow or required bending knees in order for a robot to maintain its balance or to avoid exceeding its mechanical limit.

Considering the entertainment use of humanoids, complying with the wishes of the stage director of the event on-site is essential. There must be an easy way to realize feasible bipedal walking with varied parameters such as speed, step length, and total walk length without losing the naturalness and personality of the original human motion. In previous experiments the authors were able to model a turning motion of various angles by referring to singular motion-capture data [22]. However the same procedure does not work well on walking motion. Generating a walking pattern using features extracted multiple motion-capture data was also tested with the leg module of HRP-4C [23]. This approach required so many human features that it was hard to realize on the real hardware.

III. Our Focus on Realizing Human-Like Walking

In the previous section, it was observed that an accurate imitation of human motion by a robust bipedal walking motion is very difficult. Thus we focus on only three characteristics for imitating human walking:

- Support with a toe link
- Stretched knee joint of the supporting leg
- Motion of the swing leg

To investigate human walking motion, several kinds of a female model's walking have been captured. Fig. 19 shows a sequence of photographs of the model walking during motion capturing. The model was asked to walk with a certain step length but with a free step cycle for each capturing trial. The step lengths were 0.3, 0.45, and 0.6 [m/step], and step cycles were 1.15, 0.9, and 0.83 [s/step].

The first characteristic of human walk is the existence of "single toe support", as shown in Fig. 1. The female model seems to use her toe link in order to make longer strides, a characteristic that does not appear with a short step length of 0.3 [m/step].

The second characteristic is that a human stretches the knees during the early and middle support phases, as shown in Fig. 2.

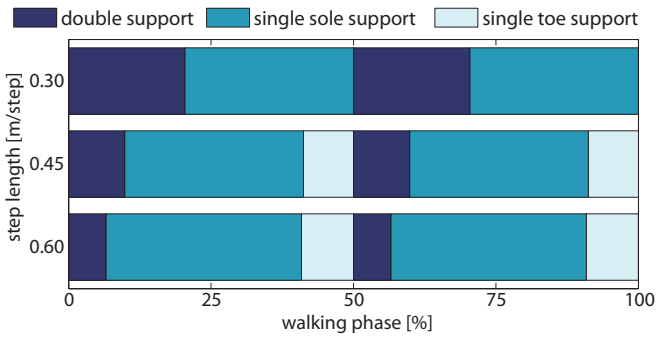

Fig. 1. Support states of the female model over a walking phase averaged among steady walking.

For the third characteristic, although it requires deep investigation on cognitive psychology or ergonomics, this paper adopts the observations taken from a psychological test to assess similarities of walking motion [15]. The observations concluded that observers tend to distinguish between walkers by their swing leg motion relative to the waist, especially those at distal ends such as the ankle and toe. Fig. 3 illustrates the position of the ankle joint relative to the hip joint, obtained by a motion-capture system.

Not only the perceptive impression but also the dynamical and mechanical constraints such as joint angle limits, maximum motor velocity, and self collision have to be taken into account. By doing so, the pattern generator, the dynamics filter, and the stabilizer are all improved. First, the pattern generator based on an analytical solution [24] is used, and modifications are done to incorporate the three characteristics of human walking motion described above. The generated motion is then filtered to become a feasible pattern [25]. Finally, the stabilizer is also improved in order to keep the ZMP [26] within the tiny support polygon during the single support phase with toe link.

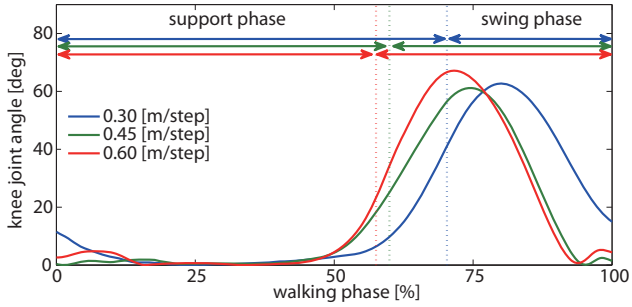

Fig. 2. Knee motion of the female model over a walking phase. The angle at 0 [deg] means the knee is fully stretched.

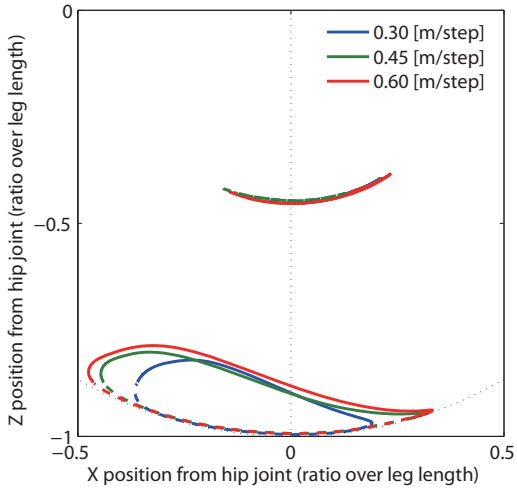

Fig. 3. Ankle and knee motion of human. The length is expressed as a ratio over leg length, which equals 1 with stretched knee joint. Solid lines signify trajectories of swing phase, and dotted lines signify those of support phase.

IV. PATTERN GENERATION

A. Conventional pattern generator

Basically, we follow the procedure of the conventional pattern generator (see [24]) in which a user gives the following inputs to generate foot motion:

- Support leg (right / left)
- Step length
- Time length of single and double support phase

According to the footprints generated using the inputs, a reference ZMP trajectory is generated using a cubic polynomial

$$p^{(j)}(t) = a_0^{(j)} + a_1^{(j)}(t-T_j) + a_2^{(j)}(t-T_j)^2 + a_3^{(j)}(t-T_j)^3 \quad (1)$$

where $p^{(j)}(t)$ is a trajectory of ZMP at time t ($T_j < t < T_{j+1}$), and the values of $a_i^{(j)}$ are the coefficients of the polynomial. The boundary T_j in each section is set as the time boundary between the single and double support phases.

The horizontal trajectory of the Center of Mass (CoM) corresponding to the reference ZMP is analytically deduced respecting the dynamics of the linear inverted pendulum model. The dynamics of a walking robot both in the sagittal plane and in the lateral plane can be approximated by the following simple equation [27]:

$$\ddot{x} = \frac{g}{z_c}(x - p) \quad (2)$$

where x is the horizontal position of the CoM, z_c is CoM height, and g is the gravity acceleration. Here z_c tentatively takes a constant value. Fig. 4 shows the generated reference CoM and ZMP trajectory in the horizontal plane.

The horizontal trajectory of the waist link is obtained by adding an offset to the reference CoM trajectory. Then inverse kinematics between the waist and foot are solved and the joint angle trajectories are obtained.

For the most part this study adopts this procedure, adding modifications in order to realize the three characteristics described in the last section.

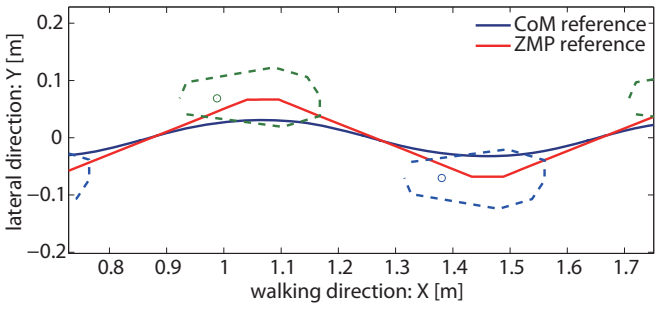

Fig. 4. Reference horizontal CoM trajectory and its reference ZMP

B. Characteristic 1: Support with a toe link

The motion of ankle and toe link is generated with cubic polynomials:

$$q_{toe}^{(k)}(t) = c_0^{(k)} + c_1^{(k)}(t-T_k) + c_2^{(k)}(t-T_k)^2 + c_3^{(k)}(t-T_k)^3 \quad (3)$$

where $q_{toe}^{k}(t)$ denotes a trajectory of a toe joint at time t ($T_k < t < T_{k+1}$), and the values of $c_i^{(k)}$ are the coefficients of the polynomial. The boundary T_k is set as the time boundary between states of the foot as shown in Fig. 5. The generated foot motion contains four states during the support phase: rotation around a heel edge, sole support, toe support, and rotation around a toe edge. Considering these states and the trajectory of the toe joints, the motion of the ankle link is determined.

However the mass distribution of a robot is not same as it is with a human. Thus the boundary T_k is not always the same as it is with human walking and needs to be determined experimentally in order to obtain a stable walking pattern. Fig. 6 compares the robot and human support phases. Even though those ratios are not exactly same, the generated walking pattern had the same support phase transition as human.

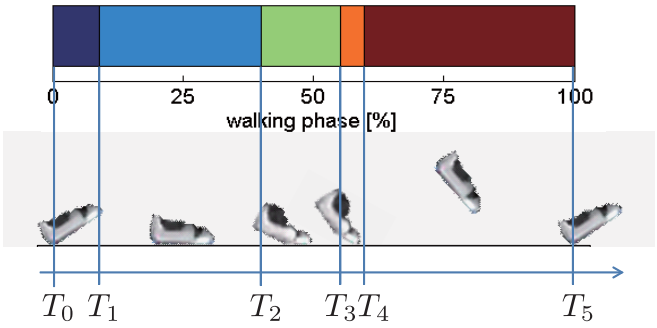

Fig. 5. Progress of the foot state. The upper bar graph shows the time ratio of human foot states. The lower images illustrate the foot states: rotation around a heel edge, sole support, toe support, rotation around a toe edge, swing, and touch down again with heel edge at 100 % of one walking cycle.

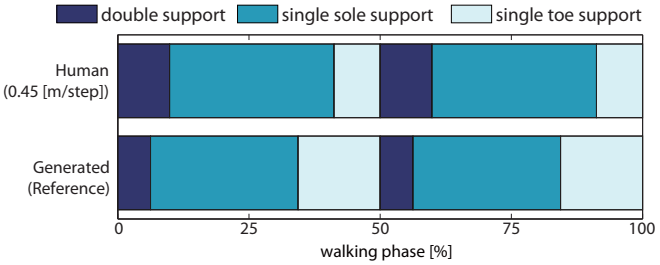

Fig. 6. Comparison of support states between human and generated pattern over a walking phase.

C. Characteristic 2: Stretched knee joint of the supporting leg

Knee joint stretching is realized by moving waist height, and the waist height is calculated by using the foot position of the support leg and the horizontal waist position.

The waist height trajectory is chosen as the trajectory that straightens the leg as much as possible unless it exceeds the maximum distance L_{max}. Using the initial waist height as shown in Fig. 7, the temporal leg length L_{tmp} is chosen according to the right and left foot motion and the waist

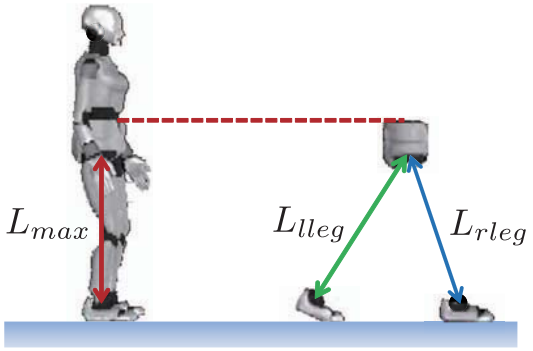

Fig. 7. Determination of leg length.

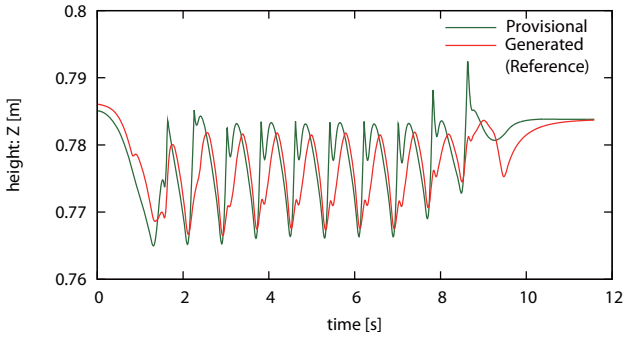

Fig. 8. Waist height trajectory. The peaky provisional height (green line) is moderated (red line).

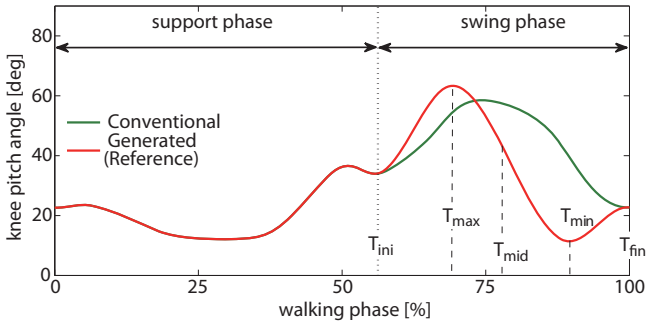

Fig. 9. Generated knee joint angle. T_{ini}, T_{max}, T_{mid}, T_{min} and T_{fin} are the interpolating points, and are determined experimentally.

trajectory:

$$L_{tmp} = \min\Big\{\max\big\{L_{rleg}, L_{lleg}\big\}, L_{max}\Big\} \qquad (4)$$

where L_{rleg} and L_{lleg} denote the distance between the right leg and the waist and between the left leg and the waist, respectively. The initial and final standing poses take L_{max} and the waist height is expressed as the offset from the temporal constant height of CoM, z_c. According to the reference horizontal position and the temporal constant height of CoM, L_{rleg} and L_{lleg} are calculated. If L_{rleg} or L_{lleg} exceeds L_{max}, the length is shortened by lowering the waist height. However, the calculated waist height trajectory has a discontinuity at the bounds of the single support and double support phase. Then it is smoothed by optimization of the waist height trajectory as the cost function with constraints of the joint angles and joint velocities of the robot. Fig. 8 shows the waist height trajectory calculated provisionally by using (4) and the smoothed one after the optimization. Fig. 9 illustrates the generated knee joint trajectory. In the middle of the support phase, it is shown that the generated knee joint angle was smaller than 20 [deg].

D. Characteristic 3: Motion of the swing leg

The swing leg pattern is generated by interpolating the joint angles of hip, knee, and ankle pitch in the swing phase by cubic polynomials. The same equation as (3) is used to generate the trajectory of these joint angles. The initial and final joint angles and velocities of the swing phase are used as boundary conditions. There are three interpolation points: minimum, maximum, and intermediate between them, and they are chosen experimentally in order to fit the human swing leg motion. The right side of Fig. 9 illustrates the generated knee joint trajectory. The knee joint initially stretches as far as its velocity would allow, then bend again to connect the next double support phase. Fig. 10 shows the spatial trajectory in the sagittal plane, comparing the conventional, proposed, and human motions. The generated swing leg pattern mostly coincided with the human trajectory and the maximum knee position in the X direction was suppressed.

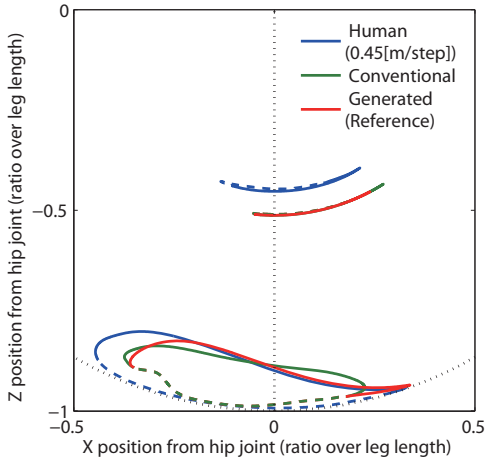

Fig. 10. Swing leg trajectory of the robot and the human's. Note that the robot and human knee positions do not coincide since the proportional lengths of upper and lower thigh differ between them.

V. DYNAMICS FILTER

It is not guaranteed that the walking pattern generated in the previous section is dynamically stable. Since it is generated regarding the robot as a single mass point, ZMP calculated using the multi-body model might be out of the support polygon. Therefore, a modification needs to be applied in order to improve dynamic stability of the pattern.

Our algorithm takes joint trajectories, feet trajectories, waist trajectory and reference ZMP trajectory as inputs and modifies joint trajectories and waist trajectory so that the

difference between the reference ZMP and a computed ZMP becomes smaller. At the beginning, we modify the waist trajectory in the horizontal plane to reduce ZMP error using a preview controller. Eventually joint trajectories are computed by solving inverse kinematics. This procedure is the same as the dynamics filter proposed in [28]. A difficulty in applying the dynamics filter to walking patterns with stretched knees is that it might be impossible to track the modified waist trajectory exactly due to joint angle and velocity limits. To cope with this difficulty, the joint trajectories are computed by a prioritized inverse kinematics solver which can handle both of equality and inequality tasks[29]. The following tasks are used in our dynamics filter.

High priority tasks: Joint angle limits, foot trajectory tracking and waist trajectory(only motion in the horizontal plane) tracking

Middle priority tasks: Waist trajectory(except motion in the horizontal plane) tracking and joint velocity limits

Low priority tasks: Joint trajectory tracking

The joint angle limits are defined as linear inequality task using *velocity damper*[25]. Since violations of joint angle limits lead to destruction of the robot hardware immediately, the joint angle limit task has the highest priority. To keep contacts with the ground properly and improve dynamics stability, foot trajectory tracking tasks and a waist trajectory(only motion in the horizontal plane) tracking task also have the highest priority. Vertical and rotational motion of the waist and joint velocity limits are maintained as far as possible. A joint trajectory tracking task is used to copy the upper body motion.

Let $\dot{\boldsymbol{q}}$ and $\dot{\boldsymbol{x}}_{ref}$ be joint velocities and reference velocities to track a given trajectory respectively. Since the trajectory tracking might have some tracking errors, it is defined using CLIK(Closed Loop Inverse kinematics)[30] technique. The task definition is

$$\boldsymbol{J}\dot{\boldsymbol{q}} = \dot{\boldsymbol{x}}_{ref} - \boldsymbol{K}\boldsymbol{e}, \tag{5}$$

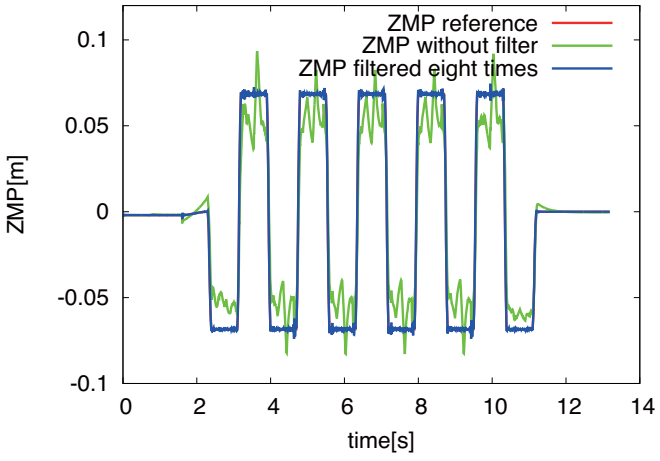

Fig. 11. Comparison of ZMP trajectories(lateral direction) with/without dynamics filtering. It's hard to see the reference ZMP trajectory because difference between it and the filtered ZMP is very small.

where $\boldsymbol{J}$, $\boldsymbol{K}$ and $\boldsymbol{e}$ are Jacobian matrix, tracking gains and errors respectively. Joint velocity limits are defined as a simple linear inequality task. At each priority level, constraints and tasks are formulated as a convex QP(Quadratic Programming) problem and solved using uQuadProg[31].

Applying the dynamics filter eight times until the average ZMP error gets the minimum, the maximum and average ZMP errors decrease from 0.106[m] and 0.019[m] to 0.022[m] and 0.001[m] respectively. We use $0.01\boldsymbol{I}$ as a tracking gain $\boldsymbol{K}$, where $\boldsymbol{I}$ is an identity matrix. Fig.11 shows comparison of ZMP trajectories in lateral direction. The initial trajectory(green) has 3[cm] errors in the middle of single support phases. These errors are reduced to less than 1[cm] by applying the dynamics filter eight times(blue). Since difference between the reference ZMP and filtered ZMP is very small, we can't see the reference ZMP(red).

VI. Stabilizer

In this section, we explain the stabilizer which controls the robot around the walking pattern generated in the former sections. Although the basic idea has already been discussed in our previous report[32], we will add an important modification to allow walking with toe supporting phase whose stability margin is extremely small.

A. Robot dynamics with ZMP control delay

To design the stabilizer, we use the same model (2) that was used for the pattern generation in IV-C. However, since the ZMP is realized by a feedback controller in our robot, it's own dynamics should be modeled. For simplicity, we assume it is the output of the first order system,

$$p = \frac{1}{1 + sT_p} p^d \tag{6}$$

where T_p is the time constant of the ZMP controller and p^d is the reference ZMP.

We model the total robot dynamics by using (2) and (6). Its validity is confirmed in our former report[32].

B. ZMP tracking control

Let us define the state vector of the delayed inverted pendulum as $\boldsymbol{x} := [x,\ \dot{x},\ p]^T$. A walking pattern generator creates a reference state $\boldsymbol{x}^{pg} := [x^{pg},\ \dot{x}^{pg},\ p^{pg}]^T$ which satisfies (2), such that

$$\ddot{x}^{pg} = \frac{g}{z_c}(x^{pg} - p^{pg}). \tag{7}$$

Then, we can regard a stabilizer as a tracking controller to let the state error $\boldsymbol{x} - \boldsymbol{x}^{pg}$ to be zero. It is done by giving the desired ZMP as follows.

$$p^d = p^{pg} + \Delta p, \tag{8}$$

where Δp is the ZMP modification for the stabilization calculated by

$$\Delta p = k_x(x^{pg} - x) + k_v(\dot{x}^{pg} - \dot{x}) + k_p(p^{pg} - p). \tag{9}$$

The state feedback gains k_x, k_v, k_p are calculated by pole assignment. We specified the poles as $(-13, -3.5, -\omega)$

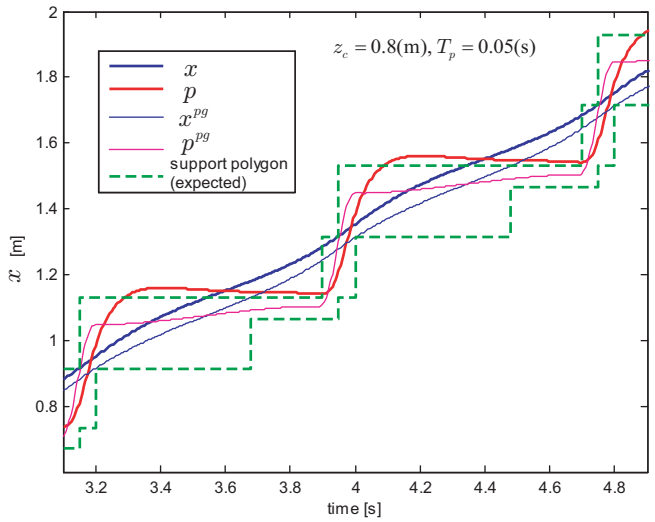

Fig. 12. Simulation of the state feedback tracking

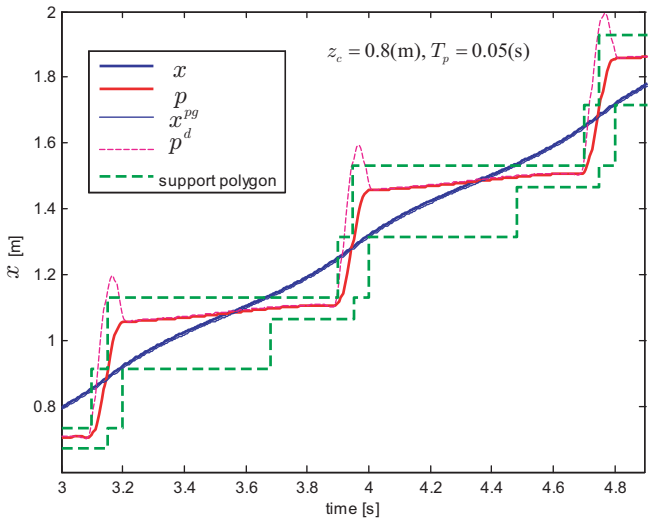

Fig. 14. Simulation of the tracking with inverse system

where $\omega := \sqrt{g/z_c}$. To obtain the maximum stability, one of the poles is set to match the eigen value of the original inverted pendulum [33]. Fig.12 shows a tracking control simulation using (8) and (9) for a reference walking pattern. We can observe large tracking errors of the CoM and the ZMP. Especially, the ZMP goes out of the expected support polygon, that means our stabilizer will not able to realize this walking pattern.

Since the tracking errors caused by the walking pattern without concerning the ZMP delay, we decided to compensate the ZMP delay by applying a filter. Instead of (8), we give the desired ZMP as

$$p^d = (1 + sT_p)p^{pg} + \Delta p, \tag{10}$$

where $(1 + sT_p)$ is an inverse system to compensate the ZMP delay. Although it is not a proper transfer function, we can design an almost equivalent filter in discrete time domain. Fig.13 shows the structure of our stabilizer with the ZMP-delay compensation. The simulation result with a controller of (9) and (10) is shown in Fig.14. We can observe the desired ZMP (dashed line) changes quickly to compensate the ZMP delay and the CoM tracks the walking pattern accurately. By this control, the desired ZMP leaves the support polygon eventually. However, it is not a problem for it is merely a control command.

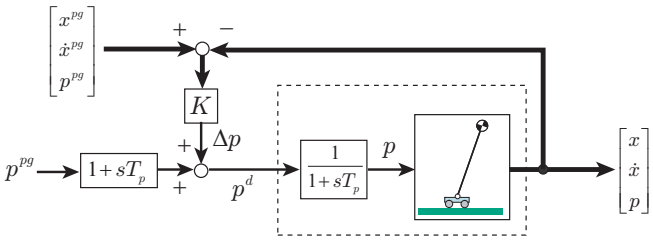

Fig. 13. Tracking controller with inverse system

VII. Experiment

A walking experiment was conducted with HRP-4C. The robot walked 4.0 [m] straight forward with 11 steps, and it took 11.6 [s]. The pattern is generated using the footprint parameters in Table I. In the table, "ss" and "ds" signify the time length of single support phase and double support phase, respectively. The step lengths were decided mainly in the reason of stabilization, but it was also considered the proportion of leg length between the human model and humanoid during 3rd to 9th step. The reference ZMP trajectory was generated interpolating two points on each footprint, using the cubic polynomial (1). Resultant trajectories are illustrated in Fig. 15. Note that the ZMP is observed to be out of the expected support polygon in the above graph of Fig. 15 (around time = 5.1, 5.9 and 6.7 [s]). This caused by the earlier touchdown of swing leg than expected at each step. Fig. 16, 17, and 18 show the three characteristics added to the walking pattern, comparing with human motion. The executed motion slightly differed from the reference motion generated the proposed pattern generator. Nevertheless, the walking motion we aimed to was successfully realized. Fig. 20 shows a sequence of photographs of HRP-4C during the walking demonstration.

TABLE I

Step length, single and double support period.

num. of step	support leg	step length [m]	ss [s]	ds [s]
1	Left	0.25	0.7	0.1
2	Right	0.35	0.7	0.1
3-9		0.40	0.7	0.1
10	Right	0.35	0.7	0.1
11	Left	0.25	0.7	0.1

VIII. Conclusions and Future Works

In this paper we aimed at realization of human-like walking with HRP-4C. An accurate imitation of human motion

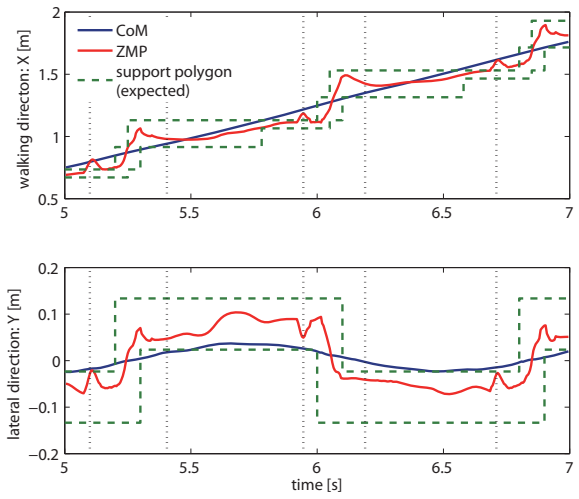

Fig. 15. Actual ZMP and CoM trajectory, and expected support polygon of the reference pattern. The dashed black lines denote the actual boundary of support phases.

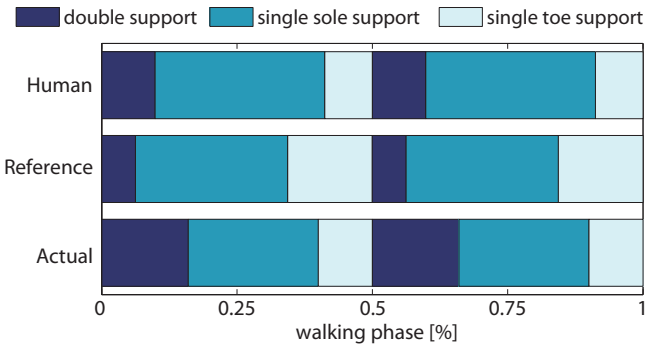

Fig. 16. Comparison of support phase ratio between human, generated reference pattern, and actual executed pattern of HRP-4C.

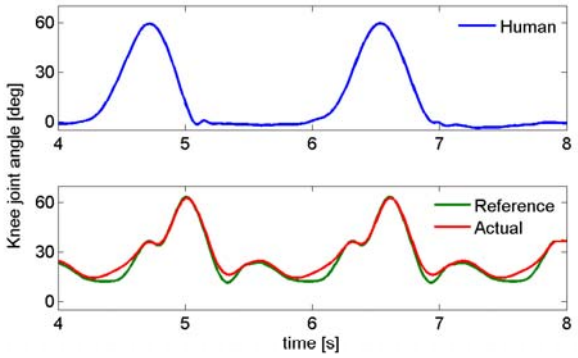

Fig. 17. Comparison of knee joint angles between human, generated reference pattern, and actual executed pattern of HRP-4C.

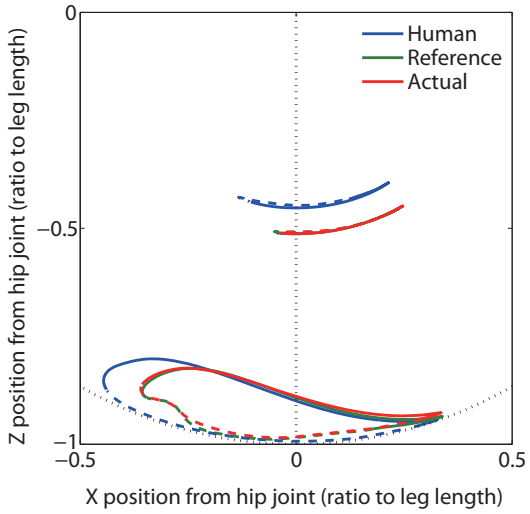

Fig. 18. Comparison of ankle and knee motion between human, generated reference pattern, and actual executed pattern of HRP-4C.

and a robust bipedal walking were however hardly realized together. Human walking characteristics to be imitated were selected not to disturb the walking feasibility: realization of single toe support, change of waist height aiming at stretched knee, modification of swing leg motion. Based on the conventional pattern generator, these characteristics were added, then generated motion was filtered to be a feasible pattern, and the stabilizer was also improved in order to keep ZMP in tiny support polygon during single support phase with toe link. Finally we successfully demonstrated the walking with HRP-4C.

Verification experiments such as a kind of Turing test are essential to guarantee that the generated motion gives an impression of naturalness or one's personality to watchers, this still warrants further investigation.

REFERENCES

[1] K. Kaneko, F. Kanehiro, M. Morisawa, K. Miura, S. Nakaoka, and S. Kajita, "Cybernetic Human HRP-4C," in *Proc. on IEEE-RAS Int. Conf. on Humanoid Robots*, 2009, pp. 7–14.

[2] K. Miura, S. Nakaoka, S. Kajita, K. Kaneko, F. Kanehiro, M. Morisawa, and K. Yokoi, "Trials of Cybernetic Human HRP-4C toward Humanoid Business," in *Proc. on IEEE Workshop on Advanced Robotics and its Social Impacts*, 2010, pp. 2010–WA01.

[3] H. I. M. Kouchi, M. Mochimaru and S. Mitani, *Anthropometric Database for Japanese Population1997-98*, Japanese Industrial Standards Center (AIST, MITI) Std., 2000.

[4] K. Kaneko, F. Kanehiro, M. Marisawa, T. Tsuji, K. Miura, S. Nakaoka, S. Kajita, and K. Yokoi, "Hardware Improvement of Cybernetic Human HRP-4C for Entertainment Use," in *Proc. on IEEE Int. Conf. on Intelligent Robots and Systems*, 2011, accepted.

[5] G. Johansson, "Visual perception of biological motion and a model for its analysis," *Perception and Psychophysics*, vol. 14, pp. 201–211, 1973.

[6] J. E. Cutting and L. T. Kozlowski, "Recognizing friends by their walk: Gait perception without familiarity cues," *Bulletin of the Psychonomic Society*, vol. 9, pp. 353–356, 1977.

[7] L. T. Kozlowski and J. E. Cutting, "Recognizing the sex of a walker from a dynamic point-light display," *Bulletin of the Psychonomic Society*, vol. 21, pp. 575–580, 1977.

[8] N. F. Troje, "Decomposing biological motion: A framework for analysis and synthesis of human gait patterns," *Journal of Vision*, vol. 2, pp. 371–387, 2002.

[9] "BiologicalMotion," http://www.biomotionlab.ca/Demos/BMLwalker.html.

[10] K. Yamane and Y. Nakamura, "Natural motion animation through constraining and deconstraining at will," *IEEE Trans. on Visualization and Computer Graphics*, vol. 9, pp. 352–360, 2003.

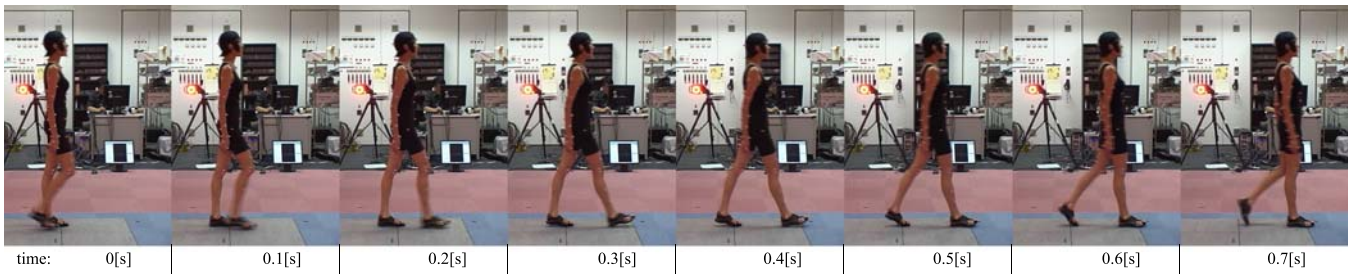

Fig. 19. A sequence of photographs of a female model walking (The model belongs to *Walking Studio Rei*).

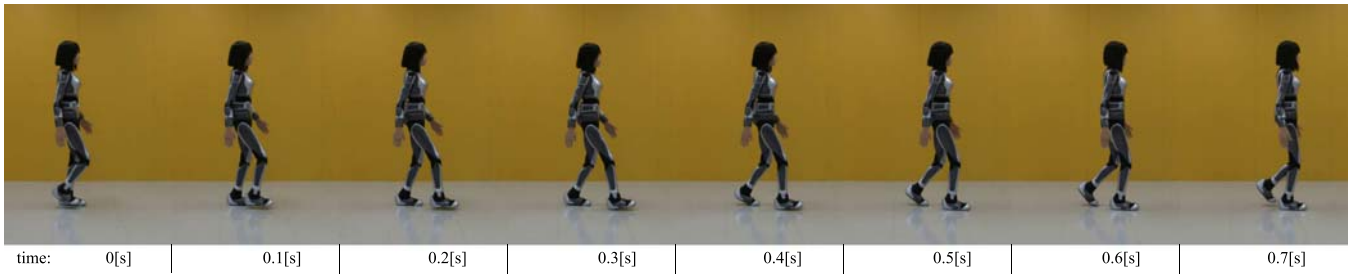

Fig. 20. A sequence of photographs of HRP-4C demonstrating generated walking pattern.

[11] A. DasGupta and Y. Nakamura, "Making Feasible Walking Motion of Humanoid Robots From Human Motioncapture Data," in *Proc. on IEEE Int. Conf. on Robotics and Automation*, 1999, pp. 1044–1049.

[12] K. Yamane and Y. Nakamura, "Dynamics filter-concept and implementation of on-line motion generator for human figures," *IEEE Trans. on Robotics and Automation*, vol. 19, pp. 421–432, 2003.

[13] O. Khatib, L. Sentis, J.-H. Park, and J. Warren, "Whole-body dynamic behavior and control of human-like robots," *Int. J. of Humanoid Robotics*, vol. 1, pp. 29–43, 2004.

[14] S. Kagami, M. Mochimaru, Y. Ehara, N. Miyata, K. Nishiwaki, T. Kanade, and H. Inoue, "Measurement and Comparison of Human and Humanoid Walking," in *Proc. on IEEE Int. Sympo. on Computational Intelligence in Robotics and Automation*, vol. 2, 2003, pp. 918–922.

[15] K. Miura, H. Furukawa, and M. Shoji, "Similarity of Human Motion: Congruity Between Perception and Data," in *Proc. on IEEE Int. Conf. on Systems, Man, and Cybernetics*, 2006, pp. 3976–3981.

[16] Y. Ogura, H. Aikawa, H. ok Lim, and A. Takanishi, "Development of a Human-like Walking Robot Having Two 7-DOF Legs and a 2-DOF Waist," in *Proc. IEEE Int. Conf. on Robotics and Automation*, 2004, pp. 134–139.

[17] Y. Ogura, K. Shimomura, H. Kondo, A. Morishima, T. Okubo, S. Momoki, H. ok Lim, and A. Takanishi, "Human-like Walking with Knee Stretched, Heel-contact and Toe-off Motion by a Humanoid Robot," in *Proc. on IEEE Int. Conf. on Intelligent Robots and Systems*, 2006, pp. 134–139.

[18] M.-S. Kim, I. Kim, S. Park, and J. H. Oh, "Realization of Stretch-legged Walking of the Humanoid Robot," in *Proc. of the IEEE-RAS International Conference on Humanoid Robots*, 2008, pp. 118–124.

[19] S. Nakaoka, A. Nakazawa, K. Yokoi, and K. Ikeuchi, "Leg Motion Primitives for a Dancing Humanoid Robot," in *Proc. IEEE Int. Conf. on Robotics and Automation*, 2004, pp. 610–615.

[20] X. Zhao, Q. Huang, Z. Peng, and K. Li, "Kinematics Mapping and Similarity Evaluation of Humanoid Motion Based on Human Motion Capture," in *Proc. on IEEE Int. Conf. on Intelligent Robots and Systems*, 2004, pp. 840–845.

[21] S. Kim, C. Kim, B. You, and S. Oh, "Stable Whole-body Motion Generation for Humanoid Robots to Imitate Human Motions," in *Proc. on IEEE Int. Conf. on Intelligent Robots and Systems*, 2009, pp. 2518–2524.

[22] K. Miura, M. Morisawa, S. Nakaoka, K. Harada, K. Kaneko, and S. Kajita, "Robot Motion Remix based on Motion Capture Data - Towards Human-like Locomotion of Humanoid Robots -," in *Proc. of the IEEE-RAS International Conference on Humanoid Robots*, 2009, pp. 596–603.

[23] K. Harada, K. Miura, M. Morisawa, K. Kaneko, S. Nakaoka, F. Kanehiro, T. Tsuji, and S. Kajita, "Toward human-like walking pattern generator," in *Proc. on IEEE/RSJ Int. Conf. on Intelligent robots and systems*, 2009, pp. 1071–1077.

[24] M. Morisawa, F. Kanehiro, K. Kaneko, N. Mansard, J. Sola, E. Yoshida, K. Yokoi, and J.-P. Laumond, "Combining Suppression of the Disturbance and Reactive Stepping for Recovering Balance," in *Proc. on IEEE Int. Conf. on Intelligent Robots and Systems*, 2010, pp. 3150–3156.

[25] F. Kanehiro, W. Suleiman, K. Miura, M. Morisawa, and E. Yoshida, "Feasible Pattern Generation Method for Humanoid Robots," in *Proc. of the IEEE-RAS International Conference on Humanoid Robots*, 2009, pp. 542–548.

[26] M. Vukobratović and J. Stepanenko, "On the Stability of Anthropomorphic Systems," *Mathematical Biosciences*, vol. 15, pp. 1–37, 1972.

[27] S. Kajita, O. Matsumoto, and M. Saigo, "Real-time 3D Walking Pattern Generation for a Biped Robot with Telescopic Legs," in *Proc. of the 2001 IEEE International Conference on Robotics & Automation*, 2001, pp. 2209–2306.

[28] S. Kajita, F. Kanehiro, K. Kaneko, K. Fujiwara, K. Harada, K. Yokoi, and H. Hirukawa, "Biped Walking Pattern Generation by using Preview Control of Zero-Moment Point," in *Proc. of the 2003 IEEE International Conference on Robotics & Automation*, 2003, pp. 1620–1626.

[29] O. Kanoun, F. Lamiraux, F. Kanehiro, E. Yoshida, J.-P. Laumond, and P.-B. Wieber, "Prioritizing Linear Equality and Inequality Systems: Application to Local Motion Planning for Redundant Robot," in *Proc. of the 2009 IEEE International Conference on Robotics & Automation*, 2009, pp. 2939–2944.

[30] P. Chiacchio, S. Chiaverini, L. Sciavicco, and B. Siciliano, "Closed-loop inverse kinematics schemes for constrained redundant manipulators with task space augmentation and task priority strategy," *International Journal of Robotics Research*, vol. 10, pp. 410–425, 1991.

[31] "uQuadProg," http://www.lis.deis.unical.it/ furfaro/uQuadProg/uQuadProg.php.

[32] S. Kajita, M. Morisawa, K. Miura, S. Nakaoka, K. Harada, K. Kaneko, F. Kanehiro, and K. Yokoi, "Biped Walking Stabilization Based on Linear Inverted Pendulum Tracking," in *Proc. on IEEE Int. Conf. on Intelligent Robots and Systems*, 2010, pp. 4489–4496.

[33] T. Sugihara, "Standing Stabilizability and Stepping Maneuver in Planar Bipedalism based on the Best COM-ZMP Regulator," in *Proc. of the 2009 IEEE International Conference on Robotics & Automation*, 2009, pp. 1966–1971.